

# PCCP

Accepted Manuscript



This is an *Accepted Manuscript*, which has been through the Royal Society of Chemistry peer review process and has been accepted for publication.

*Accepted Manuscripts* are published online shortly after acceptance, before technical editing, formatting and proof reading. Using this free service, authors can make their results available to the community, in citable form, before we publish the edited article. We will replace this *Accepted Manuscript* with the edited and formatted *Advance Article* as soon as it is available.

You can find more information about *Accepted Manuscripts* in the [Information for Authors](#).

Please note that technical editing may introduce minor changes to the text and/or graphics, which may alter content. The journal's standard [Terms & Conditions](#) and the [Ethical guidelines](#) still apply. In no event shall the Royal Society of Chemistry be held responsible for any errors or omissions in this *Accepted Manuscript* or any consequences arising from the use of any information it contains.



PCCP

PAPER

## Experimental approach to the fundamental limit on the extinction coefficients of the ultra-smooth and highly spherical gold nanoparticles<sup>†</sup>

Received 00th January 20xx,  
Accepted 00th January 20xx

DOI: 10.1039/x0xx00000x

www.rsc.org/

Dong-Kwan Kim,<sup>a</sup> Yoon Jo Hwang,<sup>b</sup> Cheolho Yoon,<sup>c</sup> Hye-On Yoon,<sup>c</sup> Ki Soo Chang,<sup>c</sup> Gaehang Lee,<sup>★cd</sup> Seungwoo Lee<sup>★ab</sup> and Gi-Ra Yi<sup>★a</sup>

The theoretical extinction coefficients of gold nanoparticles (AuNPs) have been mainly verified by analytical solving Maxwell equation for an ideal sphere, which was firstly founded by Mie (generally referred to as Mie theory). However, in principle, it hasn't been directly feasible with the experimental verification especially for the relatively large AuNPs (i.e., > 40 nm), as conventionally proposed synthetic methods have inevitably resulted in the polygonal shaped, non-ideal Au nanosphere. Here, the mono-crystalline, ultra-smooth, and highly spherical AuNPs of 40 nm–100 nm were prepared by the procedure reported in our recent work (*ACS Nano* 2013, **7**, 11064). The extinction coefficients of the ideally spherical AuNPs of 40–100 nm were empirically extracted using Beer-Lambert laws, which were then compared with theoretical limits obtained by analytical and numerical methods. The obtained extinction coefficients of the ideally spherical AuNPs herein agree much more closely with the theoretical limits, compared with those of the faceted or polygonal shaped AuNPs. Also, in order to further elucidate the importance of being spherical, we systematically compared our ideally spherical AuNPs with polygonal counterparts; effectively addressing the role of surface morphology on the spectral responses in both theoretical and experimental manners.

### Introduction

Gold nanoparticles (AuNPs) have taken lots of attraction and been investigated widely because of their potential uses in catalytic, optical, and electrical applications. For example, because of their high chemical stability and low toxicity in the biological tissue, they have been explored intensively as drug carrier or imaging agent for diagnosis.<sup>1,2</sup> Furthermore, recently, their unique optical properties (i.e., surface plasmon) promise compelling advantages in addressing one ultimate goal of nanophotonics; indeed, over the last two decades, squeezing light into the deep-subwavelength dimension through confinement near the surface of AuNPs via surface plasmon and thus inducing unnatural electric/magnetic resonance within a cluster of AuNPs (i.e., metamolecules) have been of importance in the field of nano-photonics.<sup>3</sup>

All applications described above require selective attachment of active molecules such as drug, biomolecules (e.g., DNA or protein) or imaging agents onto AuNPs via a specific chemical reaction.<sup>4-7</sup> Therefore, it is extremely important to measure the concentration of AuNPs dispersed in a solution especially for a reliable chemical reaction between AuNPs and such active molecules. In this context, there are two popular methods for measuring concentration of AuNPs relying on (i) a direct measurement of actual mass of Au atom using mass spectroscopy and (ii) a light absorption of AuNP solution using UV-Vis trans-mission spectroscopy. In mass spectroscopy, sample should be first ionized and subsequently measured by mass spectroscopy; giving us highly accurate number of AuNP in solutions. However, it generally takes long time and destroys AuNPs during the measurement. Therefore, the absorption of AuNP solution by UV-Vis spectroscopy has been more preferred in most relevant experiments, as enabling far more versatile measurement and more importantly maintaining AuNPs quality for further investigations. According to 'Beer-Lambert law', the concentration of AuNPs dispersed in solution can be exactly extracted from the solution absorbance, as follows:

$$A = \epsilon_{\text{ext}}BC \quad (1)$$

where A, B, C, and  $\epsilon_{\text{ext}}$  refer, respectively, to absorbance, the light path length of the cell used in UV-Vis spectroscopy, the concentration of AuNPs dispersed in solution ( $\text{cm}^{-1}\text{M}^{-1}$ ), and extinction coefficient. Given number of  $\epsilon_{\text{ext}}$ , both A and the

<sup>a</sup> School of Chemical Engineering, Sungkyunkwan University (SKKU), Suwon 440-746 Republic of Korea

Email: yigira@skku.edu,

<sup>b</sup> SKKU Advanced Institute of Nanotechnology (SAINT), Sungkyunkwan University (SKKU), Suwon 440-746 Republic of Korea

<sup>c</sup> Korea Basic Science Institute (KBSI), Daejeon 305-806 Republic of Korea

<sup>d</sup> University of Science and Technology, Daejeon, 305-350 Republic of Korea

<sup>†</sup> Electronic Supplementary Information (ESI) available: SEM images of gold octahedra and size distribution histograms of highly spherical AuNPs. ICP-MASS analysis of supernatant of gold octahedron suspension. Detailed descriptions for the calculation of Mie theory. Additional results of FDTD-simulated extinction coefficients of spherical AuNPs. See DOI: 10.1039/x0xx00000x

resultant C are empirically measurable, while B is fixed with respect to the measurement condition.

In principle, this measurement of concentration could be applicable to the wide range of colloidal suspensions regardless of NP material and solvent species; nevertheless, extinction coefficient itself could not be universal due to its lack of shape information. In general, the relevant optical modes of NPs such as localized surface plasmonic resonance (LSPR) or Mie (or leaky-mode) resonance is generally dependent of the shapes as well as the sizes. This aspect becomes more elucidated, when one considers the measurement of a relatively large spherical AuNPs (over 40 nm) rather than other dielectric particles. Unlike to the synthesis of dielectric NPs (silica or polystyrene), the citrate-assisted (or hydroquinone-assisted seed growth of citrate-capped AuNPs) reduction of Au chloride, which has been mostly used for the synthesis of a relatively large sized spherical AuNPs, generally results in the polygonal shapes (i.e., rough surfaces with randomly distributed facets) and shows poor reliability or yield of the synthesis. Given that the obtainable shape (or quality) of such conventional AuNPs could not be consistent, each research group working in the chemical modification of such conventional AuNPs should have their own extinction coefficients for a given size even though their values cannot be universal or may not be reliable for the sample from other batch. Indeed, several groups have tried to obtain the empirical extinction coefficients of conventional AuNPs of 3–120 nm with polydispersity in sizes and shapes; as expected, these reported values have been varied according to each research group.<sup>8,9</sup> More importantly, these reported extinction coefficients have been typically limited to a relatively smaller sized AuNPs (less than 35 nm).<sup>9</sup> Over 40 nm, the AuNPs, synthesized by such conventional methods, generally show the rough surfaces with various facets, which make it extremely difficult to measure reliable and accurate value of extinction coefficients for spherical AuNPs.

Recently, we have established a synthetic route for monodisperse, ultra-smooth, and highly spherical AuNPs (> 40nm) by advancing the experimental conditions of chemically etching the faceted Au octahedron;<sup>10</sup> unprecedented quality of these ideally spherical AuNPs with a relatively large size have been evidenced by our spectral measurements (i.e., dark-field scattering of individual AuNP or AuNP clusters) as well as the visualization through transmission electron microscope (TEM) imaging.<sup>11</sup> Our recent success raises the question of how different these ideally spherical AuNPs would be from the conventionally synthesized AuNPs especially in terms of absorbance behaviour and empirically obtainable extinction coefficients. Here, we have systematically (i) studied the UV-Vis absorbance behaviour and extinction coefficients for our ideally spherical AuNPs, which were compared with theoretical limit, (ii) rationalized the effect of the morphology of AuNP surface on the extinction behaviour by numerical simulation, and (iii) empirically compared ideally spherical AuNPs with conventional AuNP spheres in order to elucidate being importance of highly spherical. We anticipate that the empirically obtained extinction coefficients, reported in the current work, will provide a universal route to the experimental measurement of

concentration of ideally spherical AuNPs by UV-Vis absorption spectroscopy in a highly reliable and versatile way.

## Materials and Methods

### Materials

The chemicals required for the synthesis of monodisperse, ultra-smooth, and highly spherical AuNPs including ethylene glycol (EG) (anhydrous, 99.8 %), Au (III) chloride trihydrate (49.0 % metals basis), poly(dimethyldiallyl ammonium chloride) (polyDADMAC) (Mw 400,000 – 500,000, 20 wt% in H<sub>2</sub>O), phosphoric acid (PA) (85 wt% H<sub>2</sub>O), and ethanol (EtOH) (99.5 %) were purchased from Sigma-Aldrich and used as-received. For the synthesis of conventionally polygonal shaped AuNP spheres, both sodium citrate dihydrate (> 99 %, FG) and hydroquinone (> 99 %), which were also purchased from Sigma-Aldrich and used as-received, were employed in order to reduce Au chloride. The silicon wafer from Ultrasil Co. was used as a substrate for the measurement of dark-field optical microscope of AuNPs.

### Synthesis of octahedral AuNPs

A 20 mL of anhydrous EG solvent was first stirred with a magnetic bar in glass vial, and subsequently both 0.4 mL of polyDADMAC and 0.8 mL of 1 M H<sub>3</sub>PO<sub>4</sub> were added. The prepared mixture was continuously stirred for more than 5 min, and then 0.02 mL of a 0.5 M HAuCl<sub>4</sub> aqueous solution was added under continuous stirring. The mixture was maintained at room temperature for 15 min, and then the solution in the glass vial was loaded into an oil bath for 30 min, which was maintained at 195 °C throughout the reaction. During the reaction, the color of solution changed from yellow to colorless and then, gradually, to purple and finally brown. We centrifuged the solution at 13,000 rpm and dispersed the precipitates again in EtOH. This washing step was repeated at least three times to minimize the excess reactants and byproducts.

### Chemical etching process of octahedral AuNPs: toward highly spherical AuNPs

To convert the octahedral AuNPs to highly spherical counterparts, 5 μL of a 0.5 M HAuCl<sub>4</sub> solution was added into as-synthesized Au octahedral suspension at room temperature. The color of the suspension was gradually changed from brown to pink as self-evidence of conversion of octahedral to spherical geometry. Even after etching process, AuNPs are still coated with polyDADMAC, which makes AuNPs positively charged (Fig. S1). Thereby, spherical AuNPs are stably suspended in water by electrostatic stabilization.

### Synthesis of polygonal shaped AuNPs

The polygonal shaped AuNPs of a relatively large sizes (average diameter of 40 nm, 80 nm, and 100 nm) was synthesized by seed-growth of citrate coated 15 nm AuNPs.<sup>12</sup> The 15 nm sized seed AuNPs was obtained by sodium citrate-enabled reduction of Au precursor at high temperature (100 °C). First, 1 % of Au (III) chloride trihydrate (weight/volume) was added into 30 mL of ultra-pure water; then, a temperature together with

continuous stirring was increased until the solution was boiled. Once the solution was boiled, 15 mM sodium citrate aqueous solution (prepared fresh each day) was very quickly added into the solutions. After 10 min reaction under high temperature and continuous stirring, 15 nm spherical AuNPs to be used as a seed were obtained.

Before a seed-growth reaction, the 15 nm AuNPs solution was cooled at room temperature; then, an appropriated volume of such seed AuNPs solution was re-dispersed in ultra-pure water. 100  $\mu\text{L}$  of 1% Au (III) chloride trihydrate (weight/volume) was added to seed AuNP solution; subsequently, the vigorous stirring at the maximum speed without any splashing was carried out. Finally, 22  $\mu\text{L}$  of 1% sodium citrate aqueous solution (weight/volume) and 100  $\mu\text{L}$  of 0.03 M hydroquinone aqueous solution were sequentially added to the prepared AuNP seed solutions. Total volume of reaction batches was 10 mL and the size of a relatively large AuNPs was precisely controlled by adjusting the initial volume of 15 nm AuNP seed solution.

### Characterizations

The morphology of spherical and octahedral AuNPs was visualized by transmission electron microscope (TEM, Tecnai G2 F30 at 300KV) and scanning electron microscope (SEM, JEOL JSM7000F at 30KV). TEM samples were prepared by drying a droplet of dilute AuNPs on the copper grid, which is covered with a carbon film and then dried under ambient air for 1 hr. All UV-Vis spectra were measured using a double beam optics UV-Vis spectrophotometer (Optizen 3220UV) with scanning wavelength from 400 to 800 nm; the concentrations of AuNP solution were controlled by diluting the prepared AuNP solution with deionized (DI) water. An optical path length was 1 cm. The dark-field optical microscope (Nikon, Eclipse Ni series with 100 x objective lens with NA of 0.9) image of AuNPs, which were individually dispersed onto silicon substrate, was performed. During dark-field optical analysis, the linearly polarized light (p-polarization) with a proper collimation was irradiated.

### Numerical simulation & Mie scattering calculation

In order to investigate the effect of morphology of AuNPs on the extinction cross-section (light scattering + absorption), numerical simulation supported by finite-difference, time-domain (FDTD) was carried. The home-built FDTD code implemented with Drude-critical model was used<sup>13,14</sup>; the spherical AuNPs were assumed to be encapsulated by 1 nm thick polyDADMAC or citrate/hydroquinone.<sup>14</sup> The simulated results with 1 nm thick organic surfactant of AuNP were found to be well matched to the experimental results.<sup>14</sup> The complex dielectric constants of these organic surfactants were obtained by ellipsometry measurement;<sup>14</sup> the hexagonal mesh of 10 nm discretization along all direction (x-, y-, and z-axis) was employed in the model structure. The plane wave with a p-polarization and 60° incident angle was assumed to be irradiated on AuNP, which is dispersed within DI water. The absorbed and scattered light were then integrated over the solid angle of 360 degree without any restrictions on the collection angle and collected for all wavelengths of compiling spectrum. The total extinction cross section was obtained by

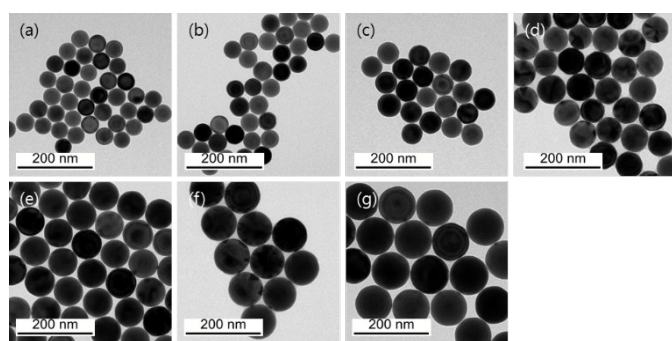
summing the obtained absorption and scattering spectrum. In addition to FDTD numerical analysis, the extinction cross section of an individual AuNP spheres was analytically calculated by solving the Maxwell equation for single spherical AuNPs, which is firstly founded by Mie (Mie or leaky-mode resonance theory),<sup>15,16</sup> Drude model (i.e., plasma frequency of  $14.3 \times 10^{15}$  rad/s, epsilon infinity of 11.85, and collision frequency of  $1.12 \times 10^{13}$  THz) was implemented in Mie resonance theory. The surrounding dielectric material was water with epsilon of 1.777 and unity of mu.

## Results and discussion

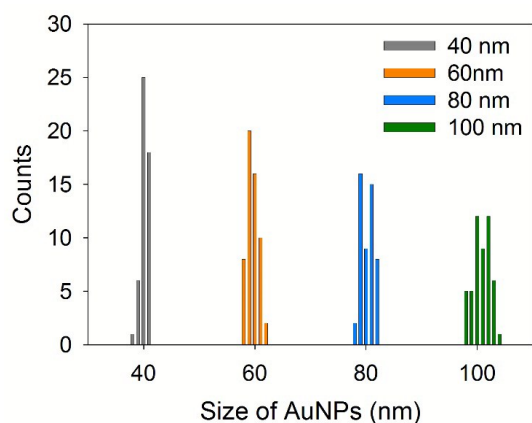
### Synthesis and characterizations of highly spherical and polygonal AuNPs

As we previously reported, the facets or edges of AuNPs (octahedral geometry) can be selectively etched by a specific chemical reaction, in which the Au atoms at the facets or edges of NPs can be removed preferentially owing to their relatively high energy or lower coordination number (number of nearest bond).<sup>17</sup> Furthermore, the size of pristine Au octahedron NPs can be highly uniform in stark contrast to other conventional AuNP spheres.<sup>10</sup> Thereby, the monodisperse, ultra-smooth (monocrystalline), and highly spherical AuNPs can become available at the moment, so as to provide an unprecedented nanomaterial platform for a deterministic and reliable engineering of plasmonic nano-optics (i.e., sophisticated engineering of electric/magnetic resonance).<sup>14,18,19</sup> Toward this direction, such ideally spherical AuNPs should be assembled into the cluster (i.e., metamolecules) with a precisely designed geometry; several self-assembly strategies including convective force or complementary binding between biological molecules (e.g., protein and DNA) have allowed for deterministic clustering of AuNPs.<sup>3,20</sup> Therefore, before assembling the clusters, AuNPs need to be decorated with such biological active molecules through a specific chemical reaction (e.g., Au-thiol bonding); for a reproducible chemical reaction, it would be essential to exactly measure AuNP extinction coefficients experimentally for various sizes, as an intermediate step in extracting the concentration of AuNPs from UV-Vis absorption spectrum. The empirical extraction of extinction coefficients of ideally spherical AuNPs was performed in three steps including (i) synthesis and characterizations of highly spherical AuNPs with various sizes, (ii) systematic analysis of extinction behaviour, and (iii) extraction of extinction coefficients.

The first step proceeded by the selective etching of edges or vertices of Au octahedra;<sup>10</sup> as a result, a set of diversely sized, highly spherical AuNPs ranging from 40 nm to 100 nm was prepared (total seven numbers of AuNP solutions with controlled sizes such as 40 nm, 50 nm, 60 nm, 70 nm, 80 nm, 90 nm, and 100 nm were prepared). The pristine Au octahedra with the controlled sizes was synthesized by polyol reduction in anhydrous EG with the presence of strongly positive-charged polyelectrolyte (i.e., polyDADMAC, used as stabilizer), as described in previous section (see SEM images of Au octahedra, summarized in Fig. S2, Supplementary Information).



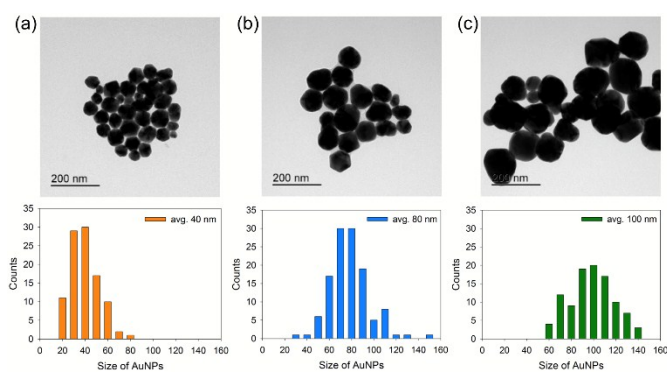
**Fig. 1.** Transmission electron microscope (TEM) images of highly spherical gold nanoparticles (AuNPs) with different sizes (a) 40 nm, (b) 50 nm, (c) 60 nm, (d) 70 nm, (e) 80 nm, (f) 90 nm, and (g) 100 nm.



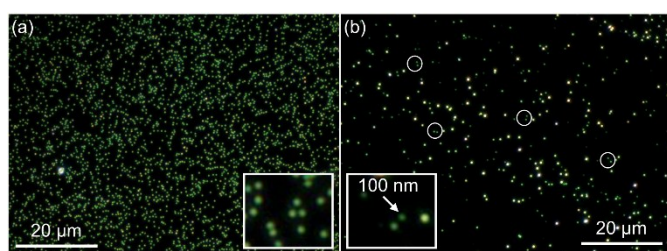
**Fig. 2.** Size distribution histograms of highly spherical AuNPs (40 nm, 60 nm, 80 nm, and 100 nm-sized AuNPs), analyzed by ImageJ software.

Fig. 1 presents the collective set of TEM images of such differently sized, highly spherical AuNPs, which were all taken with same magnification; providing us with unprecedented quality of monodisperse, ultra-smooth, and highly spherical AuNPs in a qualitative fashion. The quantitative analysis on such extremely high quality of Au-NPs can be accessed by statistic TEM image analysis, supported by open source software (i.e., ImageJ), as with our previous reports.<sup>10</sup> In Figure 2, we included the size distribution histograms of four representative highly spherical AuNPs (i.e., the sizes of 40 nm, 60 nm, 80 nm, and 100 nm) from the analysis of ImageJ; as can be seen clearly, a quite narrow distribution (less than  $\pm 5\%$ ) of AuNPs was achieved: the size distribution histograms for other AuNPs are available at Supplementary Information (Fig. S3). Gravitational height for 40-nm and 100-nm gold spheres are 684.5 and 43.8  $\mu\text{m}$ , respectively, which are higher than typical polymeric colloidal particles.<sup>21</sup>

To further elucidate the importance of being highly spherical, we also synthesized conventional AuNPs with rough surfaces and polydisperse sizes and compared their structural and optical properties with our highly spherical AuNPs. Recently, S. D. Perrault and his colleague reported the synthetic route for a relatively large-sized ( $> 50$  nm) AuNPs through citrate- and hydroquinone-assisted growth of 15 nm sized AuNP seeds;<sup>12</sup> this method has been widely used for the synthesis of the relatively large sized AuNPs. Herein, we slightly modified



**Fig. 3.** Size distribution histograms and TEM images of citrate/hydroquinone treated AuNPs (synthesized by conventional reduction/growth methods<sup>12</sup>). (a) Average size of 40 nm, (b) average size of 80 nm, and (c) average size of 100 nm.



**Fig. 4.** Dark-field optical microscope images of (a) 100 nm sized highly spherical AuNPs (the sample presented in both Fig. 1g) and (b) polygonal shaped, average 100 nm-sized AuNPs (the sample presented in Fig. 3c): White circles indicate the 100 nm-sized polygonal shaped AuNPs. Both samples were prepared onto the intrinsic silicon wafer. Insets in both (a) and (b) highlight the magnified dark-field optical microscope images.

this protocol to obtain the conventional AuNPs (average sizes of 40 nm, 80 nm, and 100 nm) to direct compare the optical behaviours. Figure 3 exhibits the TEM and ImageJ histograms of such citrate/hydroquinone-treated AuNPs; revealing a relatively wide range of size distribution ( $\approx \pm 35\%$ ) and polygonal shapes in stark contrast to our highly spherical AuNPs.

Also, we have taken the dark-field optical microscope images (Fig. 4) of 100 nm-sized highly spherical (Fig. 1g) and average 100 nm-sized polygonal shaped (Fig. 3c) AuNPs, which were dispersed onto intrinsic silicon wafer; showing more dramatic discrepancy of highly spherical AuNPs from polygonal shaped counterparts. The surprisingly even scattering colors were clearly observed within an almost given AuNPs (see Fig. 4a), whereas the polygonal shaped AuNPs showed various colours due to either their polydisperse sizes or shapes (Fig. 4b): both images were taken for same irradiation time of broadband LED white light. In addition to the uniformity of scattering colours, it is noteworthy that highly spherical AuNPs generally showed brighter scattering compared with polygonal shaped counterparts mainly due to their ultra-smooth feature together with mono-crystallinity. The effect of surface morphology on scattering behaviour was theoretically rationalized in more detail, as described in the following section.

#### Absorbance and scattering spectra

UV-Vis absorption spectra of both ideally spherical and polygonal shaped AuNPs were measured (wavelength range

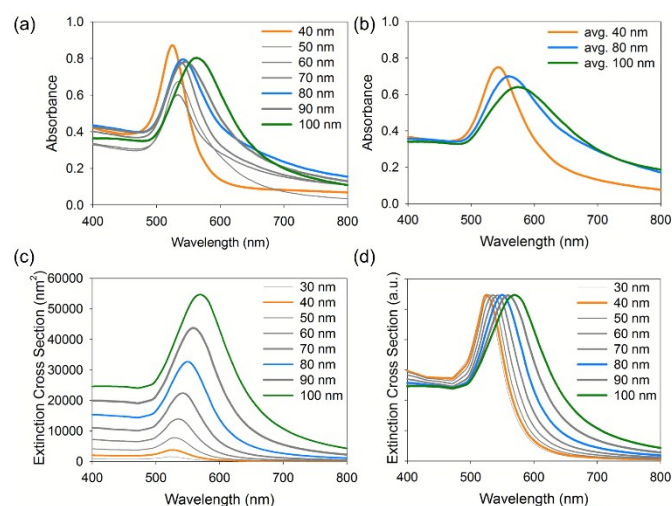


**Fig. 5.** UV-Vis spectral analysis of highly spherical and polygonal shaped AuNPs. (a) Experimentally measured UV-Vis spectra of highly spherical AuNPs (concentration is not same within the differently sized AuNPs). (b) Experimentally measured UV-Vis spectra of polygonal shaped AuNPs. (c) Theoretically calculated extinction cross sections of spherical AuNPs by Mie theory.<sup>15,16</sup> (d) The normalized extinction cross sections of spherical AuNPs, which are obtained by Mie theory.<sup>15,16</sup>

was from 400 nm to 800 nm), as summarized in Fig. 5: in these results, the concentration of each AuNPs was not even across the samples. Two important features are noteworthy. First, uniqueness of our ideally spherical AuNPs with extremely uniform size distribution was further revealed by much narrowed full width half maximum (FWHM) of the absorption peaks (Fig. 5a), compared with polygonal shaped AuNPs (Fig. 5b). Fig. 5c-d demonstrates theoretical extinction cross sections of spherical AuNPs with different sizes (original shown in Fig. 5c and normalized for clarity of FWHM and LSPR wavelength shown in Fig. 5d).

For these theoretical calculations of extinction cross sections, we used the analytical Maxwell's equation of ideally spherical AuNPs, which is established by Mie<sup>15,16</sup> and extracted total extinction cross section (light scattering + absorption). The Drude model is implemented with the variables summarized in Materials and Methods section; the employed electric permittivity of the environment ( $\epsilon_0$ ) was 1.777 (for deionized water). The detailed calculations are summarized in Supplementary Information. We can clearly observe that the extinction cross sectional behaviours of our highly spherical AuNPs agree much more closely with the theoretical values of ideal Au nanospheres, compared with those of polygonal shaped, polydisperse AuNPs.

Second, as AuNP size increases, their maximum peak was distinctly shifted to longer wavelength because the distance between electric dipole driven by LSPR is increased with AuNP size. More importantly, absorption peak for smaller particles should be sharper than one in for larger one, since the problem of optical loss at the surface of noble Au metal becomes more elucidated as with the size of NPs (also see this trend in the result of the theoretical calculation based on Mie resonance theory). As expected, our highly spherical AuNPs followed such trend of gradual increase in FWHM of peak absorption according to their size, whereas this trend was relatively dimmed in the case of

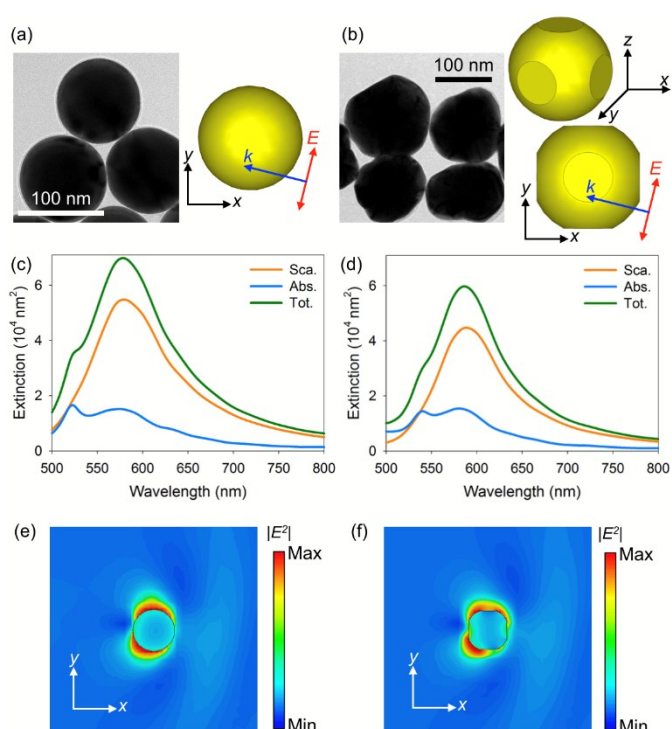


**Fig. 6.** Finite-Difference, Time-Domain (FDTD) analysis. (a-b) Schematic for the model structure and TEM images of (a) highly spherical AuNPs and (b) six-fold truncated AuNPs by 5 nm depth. (c-d) Numerically retrieved extinction cross sections of (c) highly spherical and (d) truncated AuNPs. (e-f) Simulated electric field intensity ( $|E^2|$ ) of (e) highly spherical and (f) truncated AuNPs.

polygonal shaped AuNPs. Thus, the unprecedented quality of our highly spherical AuNPs can be further identified through the UV-Vis spectral studies as with the results of dark-field optical scattering. To add analysis in more depth, the effect of morphology of AuNPs on extinction cross sectional behaviour was systematically verified by using full-field 3D numerical simulation (FDTD). Compared with analytical Mie theory, the numerical analysis powered by FDTD can reveal the effect of sophisticated surface roughness of AuNPs on extinction cross sectional behaviours with greater accuracy.

Toward this direction, we carefully approximated the model structures of polygonal shaped AuNPs by truncating spherical surface by 5 nm depths. The six truncated positions of spherical AuNPs were symmetrically arranged, as indicated in Fig. 6b; the resultant model is similar in appearance of actual polygonal shaped AuNPs (also see TEM image shown in inset of Fig. 6b). These AuNPs in the model were assumed to be dispersed in DI water; the p-polarized electric field with 60° incident angle was irradiated on the structures (see schematic in Fig. 6a-b). In particular, the induced dipole distances driven by such linear light polarization are almost same between highly spherical and polygonal shaped AuNPs, while simultaneously the pathway of dipole oscillation can be varied due to the different morphology. Fig. 6c-d presents the FDTD simulated set of (i) absorption, (ii) scattering, and (iii) total extinction (absorption + scattering) cross sections within the given model structures including 100 nm highly spherical (Fig. 6c) and truncated AuNPs (Fig. 6d). The absorption cross section is not significantly varied

with respect to the morphology, whereas scattering cross section becomes obviously reduced as spherical AuNPs are truncated. These theoretical analyses are consistent with the dark-field scattering results (Fig. 4). Such reduced scattering of AuNPs after truncating the surface originates from the inhomogeneous distribution of dipole oscillations. The truncated morphology of AuNPs forces the surface currents driven by linear polarized electric field of incident light to follow more tortuous paths; thus, hindering fluent resonant radiation, as revealed by the spatial distributions of electric field (Fig. 6e-f). This aspect should be highly dependent on both of the light incident angles and polarizations and needed to be more systematically investigated in the future works.

### Extinction coefficients

As demonstrated in the previous section, the extinction cross sectional behaviour of AuNPs should be highly dependent on their shape and polydispersity; thus, the empirical extinction coefficients of our highly spherical AuNPs should be newly established beyond those of polygonal shaped, conventional AuNPs, which have been reported so far.<sup>8,9,19</sup> Otherwise, the extracted concentration of highly spherical AuNPs solution will be inevitably over or less estimated with respect to Beer-Lambert equation (1). Toward the extraction of extinction coefficients, we have assumed two things. First, after selective etching of vertices or edges of Au octahedral (i.e., converting Au octahedra into highly-spherical AuNPs), the obtained highly spherical AuNPs was well washed (repeated centrifugal settling down and dispersing again into fresh buffer), in that both the reagents and etched Au atoms were perfectly removed from the solution. Second, during the extremely careful washing process, the amount of the converted, spherical AuNPs is assumed to be maintained without change. Meanwhile, from ICP-MS analysis of supernatant of gold octahedron suspension (Table S1, Supplementary Information), we confirmed that more than 99.95% of gold precursors (or ions) were reduced to form gold octahedron nanoparticles. Given such assumptions and confirmation, the estimated concentrations of the finally obtained, highly spherical AuNP solution can be treated as same as those of the pristine Au octahedra solution.

Consequently, in order to extract extinction coefficients with high accuracy, it is extremely important to measure the exact molar concentration of our Au octahedra or how many Au octahedra in a pristine solution in mole. In line with this, we first obtained the molar concentration of Au octahedra, which could be calculated using following equation:

$$C = N_{total} / V / N / N_{Avogadro} \quad (2)$$

where  $N_{total}$  is the amount of Au atom in Au precursor (Au chloride), which could be given according to the experimental condition of Au octahedra synthesis,  $N$  is the number of Au atoms in one octahedron,  $N_{Avogadro}$  is Avogadro number,  $V$  is volume of water in which the synthesized Au octahedra is dispersed. Herein,  $N$  can be calculated, as follow,

$$N = V * \rho / M \quad (3)$$

where  $M$  and  $\rho$  are atomic weight (187 g/mol) and density (19.4 g/cm<sup>3</sup>) of Au crystal with fcc, respectively.  $V$  is volume of octahedron (i.e.,  $(\sqrt{2}/3) \times (\text{unit side length of Au octahedra})^3$ ).<sup>22,23</sup> The volume of Au octahedra was estimated from its SEM images (see Fig. S2, Supplementary Information). Thus, the concentration of highly spherical AuNPs can be calculated: once the absorption of highly spherical AuNPs is experimentally obtained, we could extract the extinction coefficients according to Beer-Lambert equation (1). In experimental measurement of UV-Vis spectroscopy, the suspension of highly spherical AuNPs was diluted for a better signal in UV-Vis spectroscopy. Generally, in our experiments, few tens of nano molar concentration of highly spherical AuNPs has been obtained after washing process; such highly concentrated and spherical AuNP solution showed the absorption over unity at the peak of LSPR. Thereby, for a high accuracy, such AuNP solution was diluted to adjust the concentration to be tens of pico molar level. Table 1 summarizes the extracted extinction coefficients of highly spherical AuNPs with different sizes (third column).

**Table 1.** The theoretically calculated extinction coefficients of a spherical AuNPs with different sizes (by FDTD and Mie theory in 1st and 2nd column); the empirically extracted extinction coefficients of highly spherical (3rd column) and polygonal shaped (4th column) AuNPs.

size (nm)	FDTD simulation (M <sup>-1</sup> cm <sup>-1</sup> )	Mie theory (M <sup>-1</sup> cm <sup>-1</sup> )	Highly spherical AuNPs (M <sup>-1</sup> cm <sup>-1</sup> )	Polygonal shaped AuNPs (M <sup>-1</sup> cm <sup>-1</sup> )
40	3.35 × 10 <sup>10</sup>	9.85 × 10 <sup>9</sup>	6.73 × 10 <sup>9</sup>	1.01 × 10 <sup>8</sup>
50	5.81 × 10 <sup>10</sup>	2.02 × 10 <sup>10</sup>	1.39 × 10 <sup>10</sup>	-
60	8.36 × 10 <sup>10</sup>	3.63 × 10 <sup>10</sup>	2.31 × 10 <sup>10</sup>	-
70	11.24 × 10 <sup>10</sup>	8.53 × 10 <sup>10</sup>	3.85 × 10 <sup>10</sup>	-
80	14.09 × 10 <sup>10</sup>	10.21 × 10 <sup>10</sup>	5.54 × 10 <sup>10</sup>	1.82 × 10 <sup>9</sup>
90	16.52 × 10 <sup>10</sup>	11.43 × 10 <sup>10</sup>	8.30 × 10 <sup>10</sup>	-
100	18.40 × 10 <sup>10</sup>	14.30 × 10 <sup>10</sup>	9.74 × 10 <sup>10</sup>	5.42 × 10 <sup>9</sup>

We compared these obtained extinction coefficients of our highly spherical AuNPs with the theoretically calculated extinction coefficients. First, the theoretical values of extinction cross sections at each LSPR resonance were obtained by both Mie theory and FDTD analyses. Then, these theoretically obtained extinction cross sections can be converted into extinction coefficients, as follows:

$$C_{ext} = 0.2302 \epsilon_{ext} / N_{Avogadro} \quad (4)$$

where  $C_{ext}$  is extinction cross section. Table 1 presents the calculated extinction coefficients ( $\epsilon_{ext}$ ) by FDTD simulation (1st column) and analytical Mie theory (2nd column): extinction spectral results of 40–100 nm sized AuNPs simulated by FDTD are summarized in Fig. S4, Supplementary Information (extinction for 100 nm sized spherical AuNPs is presented in Fig. 6d). It is important to note that the measured extinction coefficients of our highly spherical AuNPs (3rd column) were found to be comparable or slightly smaller than the theoretical counterparts (see Table 1): the theoretical values (e.g., Mie theory) are typically 1.46 times higher than the empirical values (this difference was less than an order of magnitude).

Meanwhile, the empirically obtained extinction coefficients of polygonal shaped AuNPs can further elucidate the unprecedented quality of our highly spherical AuNPs. As with the results of highly spherical AuNP concentration and other relevant works,<sup>9,12</sup> we assumed that 100 % of Au precursor (Au chloride) was consumed and converted into face-centered cubic structure (fcc) AuNPs; the polygonal shaped AuNPs were simplified to be a sphere with average diameter. Thereby, number of Au atoms ( $N$ ) in one polygonal shaped AuNP can be approximated as follows:

$$N = (\pi/6)(\rho D^3/M) \quad (5)$$

where  $D$  is the diameter of fcc AuNP. Table 1 (4th column) summarizes empirical extinction coefficients of polygonal shaped AuNPs with average diameter of 40 nm (Fig. 3a), 80 nm (Fig. 3b), and 100 nm (Fig. 3c). From the results, the obtained extinction coefficients of highly spherical AuNPs found to be at least on order of magnitude higher than those of polygonal shaped AuNPs, which is consistent with the results in Fig. 4-5.

We then checked the sensitivity of absorption change to the concentration of highly spherical and polygonal shaped AuNPs (Fig. 7). As clearly observed, the higher extinction coefficients of highly spherical AuNPs were further reflected by the enhanced sensitivity of absorption change to the concentration compared with those of polygonal shaped AuNPs

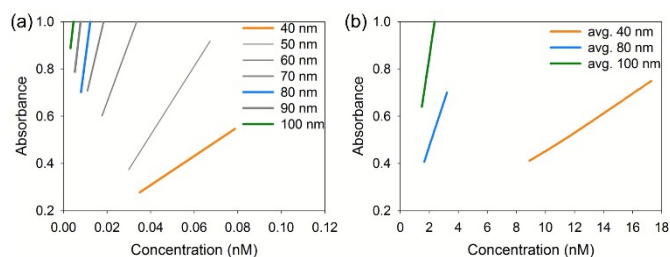


Fig. 7. The absorption sensitivity of (a) highly-spherical and (b) polygonal-shaped AuNPs to the concentration change.

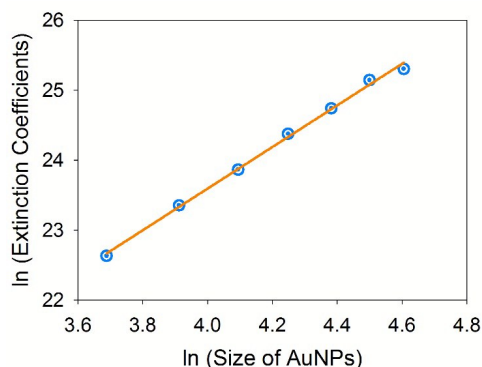


Fig. 8. The double logarithm plot of extinction coefficients versus the size of highly spherical AuNPs.

Finally, we profiled the double logarithm of extinction coefficients versus sizes of highly spherical AuNPs, as presented in Fig. 8. Obviously, the good linear fitting of natural logarithm

of extinction coefficients against the sizes of highly spherical AuNPs was achieved (i.e.,  $\ln \epsilon_{\text{ext}} = k \ln D + \alpha$ , where  $k$  and  $\alpha$  were 2.975 and 11.692, respectively). The linear correlation coefficient was 0.9972, as in accordance with the Mie theory.<sup>15,16</sup> Other groups reported a quite similar trend with the citrate-, decanethiol-, and oleylamine-capped AuNPs; this means that the extinction behaviour of AuNPs is mainly dependent on the shapes and sizes regardless of a surfactant species. This is because the thickness of surfactants is generally 1–2 nm, far much thinner than sizes of AuNPs.

## Conclusions

A series of monodisperse, ultra-smooth, and highly spherical AuNPs of 40–100 nm was prepared by selective chemical etching of Au octahedral vertices or edges. Then, their extinction coefficients for each different size were empirically obtained using Beer-Lambert law from UV-Vis absorption spectra. The extinction coefficients of our ideally spherical AuNPs were higher, compared with polygonal shaped AuNPs and closely approached to the theoretical limits (e.g., Mie theory). Therefore, we believe that our extinction coefficients measured in this study could be used for future experimental investigation using Au nanospheres without much modification.

## ACKNOWLEDGMENTS

This work was supported by Samsung Research Funding Center for Samsung Electronics under Project Number SRFC-MA1402-09.

## References

- 1 E. E. Connor, J. Mwamuka, A. Gole, C. J. Murphy, M. D. Wyatt, *Small*, 2005, **1**, 325-327.
- 2 P. Ghosh, G. Han, M. De, C. K. Kim, V. M. Rotello, *Adv. Drug Deliv. Rev.*, 2008, **60**, 1307-1315.
- 3 J. A. Fan, C. Wu, K. Bao, J. Bao, R. Bardhan, N. J. Halas, V. N. Manoharan, P. Nordlander, G. Shvets, F. Capasso, *Science*, 2010, **328**, 1135-1138.
- 4 G. Han, C. C. You, B. J. Kim, R. S. Turingan, N. S. Forbes, C. T. Martin, V. M. Rotello, *Angew. Chem. Int. Ed.*, 2006, **45**, 3165-3169.
- 5 H. Wang, Y. Chen, X. Y. Li, Y. Liu, *Mol. Pharmaceutics*, 2007, **4**, 189-198.
- 6 P. S. Ghosh, C. K. Kim, G. Han, N. S. Forbes, V. M. Rotello, *ACS Nano*, 2008, **2**, 2213-2218.
- 7 R. Hong, G. Han, J. M. Fernandez, B. J. Kim, N. S. Forbes, V. M. Rotello, *J. Am. Chem. Soc.*, 2006, **128**, 1078-1079.
- 8 W. Haiss, N. T. Thanh, J. Aveyard, D. G. Fernig, *Anal. Chem.* 2007, **79**, 4215-4221.
- 9 X. Liu, M. Atwater, J. Wang, Q. Huo, *Coll. & Surf. B* 2007, **58**, 3-7.
- 10 Y. J. Lee, N. B. Schade, L. Sun, J. A. Fan, D. R. Bae, M. M. Mariscal, G. Lee, F. Capasso, S. Sacanna, V. N. Manoharan, G.-R. Yi, *ACS Nano*, 2013, **7**, 11064-11070.
- 11 J. A. Fan, K. Bao, J. B. Lassiter, J. Bao, N. J. Halas, P. Nordlander, F. Capasso, *Nano Lett.* 2012, **12**, 2817-2821.
- 12 S. D. Perrault, W. C. W. Chan, *J. Am. Chem. Soc.*, 2009, **131**, 17042-17043.
- 13 S. Lee, J. Kim, *Appl. Phys. Express*, 2014, **7**, 112002.

## ARTICLE

PCCP

- 14 M. Kim, S. Lee, J. Lee, D. K. Kim, Y. J. Hwang, G. Lee, G.-R. Yi, Y. J. Song, *Opt. Express* 2015, **23**, 12766-12776.
- 15 S. Link, Z. L. Wang, M. A. El-Sayed, *J. Phys. Chem. B* 1999, **103**, 3529-3533.
- 16 G. Mie, *Ann. Phys. (Leipzig)*, 1908, **25**, 377-445.
- 17 S. Hong, K. L. Shuford, S. Park, *Chem. Mater.*, 2011, **23**, 2011-2013.
- 18 J. A. Fan, K. Bao, C. Wu, J. Bao, R. Bardhan, N. J. Halas, V. N. Manoharan, G. Shvets, P. Nordlander, F. Capasso, *Nano Lett.*, 2010, **10**, 4680-4685.
- 19 S. Mühlig, C. Rockstuhl, V. Yannopapas, T. Bürgi, N. Shalkevich, F. Lederer, *Opt. Express*, 2011, **19**, 9607-9616.
- 20 S. N. Sheikholeslami, H. Alaeian, A. L. Koh, J. A. Dionne, *Nano Lett.* 2013, **13**, 4137-4141.
- 21 V. Prasad, D. Semwogerere, E. R Weeks, *J. Phys.: Condens. Matter*, 2007, **19**, 113102.
- 22 A. S. Barnard, N. P. Young, A. I. Kirkland, M. A. van Huis, H. Xu, *ACS Nano*, 2009, **3**, 1431-1436.
- 23 P. K. Jain, K. S. Lee, I. H. El-Sayed, M. A. El-Sayed, *J. Phys. Chem. B* 2006, **110**, 7238-7248.